

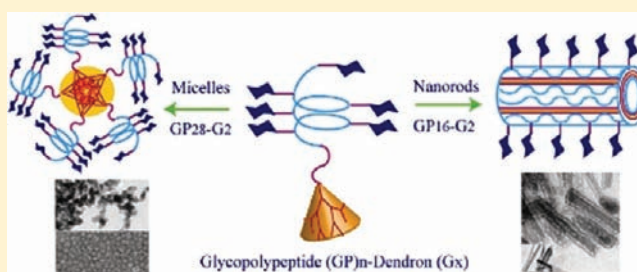
# Multiple Topologies from Glycopolyptide–Dendron Conjugate Self-Assembly: Nanorods, Micelles, and Organogels

Debasis Pati,<sup>†</sup> Nagendra Kalva,<sup>‡</sup> Soumen Das,<sup>†</sup> Guruswamy Kumaraswamy,<sup>‡</sup> Sayam Sen Gupta,<sup>\*,†</sup> and Ashootosh V. Ambade<sup>\*,‡</sup>

<sup>†</sup>CRcST Chemical Engineering Division and <sup>‡</sup>Polymer Science and Engineering Division, National Chemical Laboratory, Pune 411008, India

**S** Supporting Information

**ABSTRACT:** Glycopolyptides (GPs) were synthesized by ring-opening polymerization of glycosylated *N*-carboxyanhydride monomer and attached to hydrophobic dendrons at one chain end by “click” reaction to obtain amphiphilic anisotropic macromolecules. We show that by varying polypeptide chain length and dendron generation, an organogel was obtained in dimethylsulfoxide, while nanorods and micellar aggregates were observed in aqueous solutions. Assemblies in water were characterized by electron microscopy and dye encapsulation. Secondary structure of the GP chain was shown to affect the morphology, whereas the chain length of the poly(ethylene glycol) linker between the GP and dendron did not alter rod-like assemblies. Bioactive surface chemistry of these assemblies displaying carbohydrate groups was demonstrated by interaction of mannose-functionalized nanorods with ConA.



## INTRODUCTION

Glycopolymers, viz. synthetic polymers with carbohydrate moieties in the side chain, have been of immense interest to the field of tissue engineering and drug delivery.<sup>1</sup> This interest stems from the fact that carbohydrates play complex roles *in vivo*, particularly in biomolecular recognition events such as cellular recognition, cancer cell metastasis, and inflammation.<sup>2</sup> Polyvalent interactions between lectins and carbohydrates mediate such processes that can be mimicked by using glycopolymers. Since glycopolymers typically have several pendant carbohydrate groups they are polyvalent and can simultaneously bind to several lectins, thus enhancing their affinity and selectivity for lectins many-fold. For glycopolymers to be used as delivery vehicles and as biomaterials, it would be advantageous if they could be assembled into supramolecular nanostructures that can be tuned to appropriately display their carbohydrate moieties. Thus, amphiphilic block copolymers containing glycopolymers as one of their blocks represent an interesting motif to build self-assembled nanostructures.<sup>3</sup> For example, glucose-grafted polybutadiene-*block*-polystyrene was shown to self-assemble into vesicles in organic as well as aqueous media.<sup>3a</sup> However, synthetic glycopolymers<sup>4</sup> typically do not form well-defined secondary structures, and that may render them less effective for biological recognition processes.<sup>5</sup> On the other hand, glycopolyptides (GPs), wherein sugar units are attached to a polypeptide backbone, mimic the molecular composition of proteoglycans and have been demonstrated to fold into well-defined secondary structures (e.g.,  $\alpha$ -helix), which allows ordered display of the carbohydrate moieties.<sup>6</sup> Hence, they represent suitable candidates for

biological applications. This has led to a surge in reports on their synthesis.<sup>7</sup> Here, we combine the advantages of GPs with the microstructural tunability conferred by a block copolymer architecture and demonstrate that such systems assemble into macromolecular assemblies whose geometry is determined by parameters that characterize the block copolymer, such as chain length and backbone conformation. Only one report recently appeared on multiple morphologies obtained from poly( $\gamma$ -benzyl-L-glutamate)-*block*-poly(galactosylated propargylglycine) amphiphilic block copolymers by varying the GP content.<sup>8</sup>

Here we report the synthesis and self-assembly of GP–dendron conjugates for the first time, where dendrons are perfectly branched, wedge-shaped molecules. Our work is inspired by previous reports of dendron-containing macromolecules where the hydrophobicity of the dendron drives phase separation and macromolecular assembly at low polymer concentrations, while non-covalent interactions between the other block and structural asymmetry guide the self-assembly.<sup>9</sup> Dendron-containing macromolecules is a broad class that includes linear–dendritic copolymers, wherein linear polymer chains are attached to the periphery and/or focal point of the dendron, and dendron–rod and dendron–rod–coil type molecules, wherein a rigid-rod-like small molecule is attached to the focal point of a dendron that is further connected to a linear polymer in the latter case. We hypothesized that the

Received: January 4, 2012

Revised: April 15, 2012

Published: April 16, 2012

highly anisotropic molecular architecture realized from attaching a dendron to one chain end of a GP would provide an interesting motif to investigate self-assembly. We prepared an amphiphilic block copolymer comprising a linear hydrophilic GP block with significant helicity, connected through a flexible amphipathic poly(ethylene glycol) (PEG) linker to a perfectly branched hydrophobic dendron (Figure 1; Table 1). We

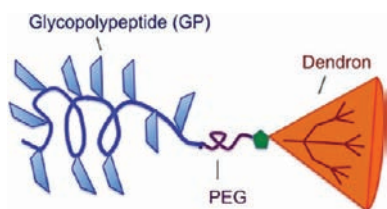


**Figure 1.** Schematic representation of glycopolyptide–dendron conjugates.

selected the gallate benzyl ether dendron with long alkyl chains so that the GPs will be relatively polar, conferring the amphiphilicity necessary for block copolymer assembly. Given the chemical and structural anisotropy in these block copolymers, we anticipate a strong tendency toward micro-phase segregation between the blocks. Our choice for the block copolymer allows us to independently tune (i) the size of the hydrophobic dendron (by varying the number of generations) as well as (ii) the chain length and (iii) amphiphilicity of the polar GP (due to the protecting groups on the sugar residues). Finally, we can also independently vary the secondary structure in the polypeptide backbone and length of the PEG linker. We demonstrate that varying the molecular attributes of the GP–dendron block copolymer selectively affords various glycosylated morphologies, such as micelles, nanorods, and gels.

## EXPERIMENTAL SECTION

**Materials and Methods.** Details on the synthesis of monomers and polymers are given in the Supporting Information. FT-IR spectra were recorded on a Perkin-Elmer FT-IR spectrometer GX instrument by making KBr pellets. Pellets were prepared by mixing 3 mg of sample with 97 mg of KBr.  $^1\text{H}$  NMR spectra were recorded on Bruker spectrometers (200, 400, or 500 MHz).  $^{13}\text{C}$  NMR and DEPT spectra were recorded on Bruker spectrometers (50, 100, or 125 MHz), and relative signals are reported according to deuterated solvent used. Size-exclusion chromatography of the GPs was performed using an instrument equipped with a Waters 590 pump and a Spectra System RI-150 RI detector. Separations were effected by  $10^5$ ,  $10^3$ , and 500 Å Phenomenex 5  $\mu\text{m}$  columns using 0.1 M LiBr in DMF eluent at 60 °C, at sample concentrations of 5 mg/mL. A constant flow rate of 1 mL/min was maintained, and the instrument was calibrated using polystyrene standards. Polydispersity index (PDI) values were calculated using WinGPC software. Circular dichroism (190–260 nm) spectra of the GPs (0.25–1.0 mg/mL in acetonitrile or deionized water) were recorded (JASCO CD spectropolarimeter, model J-815) in a cuvette with 1 mm path length. All the spectra were recorded for an average of three scans and are reported as a function of molar ellipticity  $[\theta]$  vs wavelength. Small-angle X-ray scattering (SAXS) measurements were performed on a Bruker Nanostar instrument equipped with a rotating anode and a 2D wire detector, used over a  $q$ -range of 0.01–0.20 Å $^{-1}$ . An LSM 710 Carl Zeiss laser scanning confocal microscope was used to image the fluorescent organogel using a He–Ne laser (543 nm) and an argon ion laser (488 and 514 nm) for our experiments. Transmission electron microscopy (TEM) measurements were done at 100 kV on an FEI Technai F20 instrument. Samples were imaged using a Quanta 200 3D scanning electron microscope (SEM). Prior to SEM imaging, the sample was

sputter-coated using a Polaron SC 7630 sputter-coater, giving Au thickness of 5 nm on the sample.

**General Procedure for the Synthesis of GP–Dendron Conjugates by “Click Reaction”.** To a solution of azide-PEG end-functionalized acetyl (Ac)-protected GP in tetrahydrofuran (THF)/methanol/water (2:1:0.2) was added alkynyl-dendron (1.5 equiv), and the resultant reaction mixture was degassed by three freeze–pump–thaw cycles.  $\text{CuSO}_4$  (0.2 equiv) and sodium ascorbate (0.4 equiv) were then added, and the reaction was allowed to proceed for 24 h under argon atmosphere. The progress of the reaction was monitored by the disappearance of the azide stretch at 2115  $\text{cm}^{-1}$  in FT-IR. After completion of the reaction, the solvent was removed under reduced pressure. The reaction mixture was dissolved in ethyl acetate and washed multiple times with aqueous ammonia solution to remove the copper salt. The solvent was then evaporated completely under reduced pressure. Excess dendron alkyne (G1 and G2) was removed by multiple washings with mixed solvent (ethyl acetate:hexane = 0.1:0.9). The off-white compounds were dried under vacuum overnight at 45 °C to afford GP–dendron copolymers.

**Deprotection Procedure for the GP–Dendron Conjugates.** Hydrazine monohydrate (25 equiv) was added to the solutions of all the Ac-protected GP–dendrons in THF (10 mg/mL), and the reactions were stirred for 7–8 h at room temperature. Reactions were quenched by addition of acetone, and then solvent was removed completely under reduced pressure. The solid residues were dissolved in a mixture of dimethylsulfoxide (DMSO) and deionized water (1:1) and transferred to dialysis tubing (3.5 and 12 kDa molecular weight cutoff according to polymer molecular weight). The samples were dialyzed against deionized water for 3 days and lyophilized to yield GP–dendron copolymers as white solids in 70% yield.

**General Procedure for Self-Assembly of Deprotected GP–Dendron Copolymers in Water.** Fully deprotected polymers ( $n\text{GP-G}_x$ ) were dissolved in DMSO and diluted to DMSO:water = 1:1 by dropwise addition of water with stirring to obtain final concentration of 0.1 wt %. The resulting suspension was dialyzed thoroughly against deionized water using 12 kDa cellulose membrane for 2 days, changing the water every 3 h to obtain a clear, translucent solution in pure water.

## RESULTS AND DISCUSSION

**Synthesis of GP–Dendron Copolymers.** We recently reported a simple and versatile methodology for synthesis of GPs via ring-opening polymerization of a carbohydrate-appended *N*-carboxyanhydride (NCA).<sup>10</sup> This method assures incorporation of sugar residues on every repeat unit. Using our procedure, azide-PEG-terminated GPs of two different chain lengths (DP = 16, 28; calculated from  $^1\text{H}$  NMR) based on poly-*L*-lysine with pendant Ac-protected *D*-glucose were synthesized. The ratio of weight fractions of hydrophobic and hydrophilic blocks is an important parameter used to control block copolymer morphology.<sup>11</sup> Hence, the chain lengths were targeted based on considerations of the hydrophilic–lipophilic balance (HLB) so that the weight fraction of hydrophobic (dendron) part in our polymers does not exceed 26%. The azide-functionalized GPs (Ac16GP- $\text{N}_3$  and Ac28GP- $\text{N}_3$ ) and dendrons up to second generation (G1 and G2) with alkyne at the focal point were clicked together using the [3+2] copper-catalyzed azide–alkyne cycloaddition (CuAAC) reaction. This reaction, often called “click reaction”, has emerged as an important tool for preparation of novel polymeric architectures.<sup>12</sup> Four different Ac-protected GP–dendron conjugates were obtained, described henceforth as Ac16GP-G1, Ac28GP-G1, Ac16GP-G2, and Ac28GP-G2. Structures of these polymers are shown in Table 1. The obtained GP–dendron copolymers were characterized by NMR, IR, and GPC techniques to ascertain the structural integrity and purity

Table 1. Structural Parameters of Glycopolyptide–Dendron Copolymers

Polymer Name RnGP-Gx <sup>a</sup>	R	sugar residue	m	Structure of the Polymer
Ac16GP-G1	Ac	$\beta$ -glucose	11	
Ac28GP-G1	Ac	$\beta$ -glucose	11	
16GP-G1	H	$\beta$ -glucose	11	
28GP-G1	H	$\beta$ -glucose	11	
Ac16GP-G2	Ac	$\beta$ -glucose	11	
Ac28GP-G2	Ac	$\beta$ -glucose	11	
16GP-G2	H	$\beta$ -glucose	11	
28GP-G2	H	$\beta$ -glucose	11	
<i>manno</i> 14GP-G2	H	$\alpha$ -mannose	11	
<i>manno</i> 28GP-G2	H	$\alpha$ -mannose	11	
14GP-HEG-G2	H	$\beta$ -glucose	6	
16GP-TEG-G2	H	$\beta$ -glucose	2	

<sup>a</sup>*n* = GP chain length, R = Ac or H.

(Supporting Information, Figures S1, S2, and S10–S48; Table S1).

**Assembly of Protected GP–Dendron Copolymers in Organic Solvent.** All acetylated polymers were soluble in common organic solvents. Interestingly, when a 0.7 wt % clear solution of Ac16GP-G2 in acetonitrile was left for a few minutes at room temperature, it turned into a gel that did not flow on inverting a tube of 1 cm diameter (viz. the yield stress exceeded  $\sim 20$  Pa). Gelation was observed only for Ac16GP-G2, which had the highest weight fraction of the hydrophobic part (19.4%). On the other hand, 0.7 wt % solution of Ac28GP-G2 and both the G1-attached GPs (Ac16GP-G1 and Ac28GP-G1) did not gel, indicating that increased hydrophilicity in the amphiphilic GP does not lead to gelation.

Packing of  $\alpha$ -helical chains by noncovalent interactions has been suggested as a driving force for polypeptide self-assembly into polymersomes and sheet-like structures.<sup>3b,13</sup> We hypothesized that, in polar aprotic solvent such as acetonitrile, gelation could be driven by hydrophobicity of dendrons that is further aided by packing of helical GP chains. Since both components take part in intermolecular interactions, a physically cross-linked network is obtained rather than isolated self-assembled structures, which results in a gel. The microstructure of the gel was further investigated by confocal scanning microscopy of a gel formed by fluorescently labeled Ac16GP-G2, which shows a network of fibers typical of gels (Figure 2A). SAXS analysis provides further insight into the local structure of the gel fibers (Figure 2B). The envelope of scattering curve decays with a



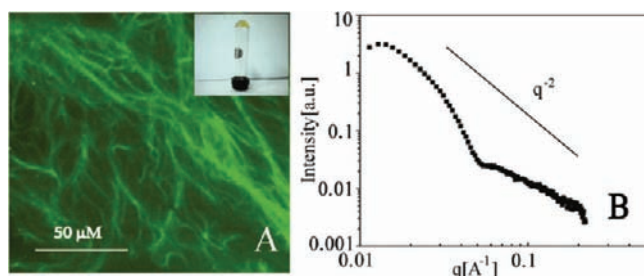


**Figure 2.** (A) Confocal microscopy image of the gel from a fluorescently labeled Ac16GP-G2. Inset: picture of the gel in inverted tube. (B) SAXS data for 1 wt % Ac16GP-G2 in acetonitrile.

power law of  $q^{-2}$ , suggesting that the GP–dendron block copolymers might organize into locally flat sheet-like structures. While this structural interpretation is not unambiguous,<sup>14</sup> it is consistent with scanning electron micrographs of freeze-dried assemblies of the block copolymers (Figure S4A).

**Assembly of Deprotected GP–Dendron Copolymers in Aqueous Solution.** The promise of glycopolymers is fully realized when the carbohydrate moieties are in the deprotected form so that they can bind biological targets. Toward this goal, all the polymers were deacetylated using hydrazine hydrate to obtain  $n$ GP-G $x$  that were now truly amphiphilic, with carbohydrate moieties carrying OH groups. Evidence for the presence of secondary structure in the GP component was obtained from CD spectra that showed a peak at 222 nm, typical of helical polypeptides (Figure S3B). Interestingly, gelation was observed after deprotection also in a more polar and aprotic solvent, viz. DMSO. There are several examples of organogels in DMSO, and intermolecular hydrogen bonding has been suggested as the mechanism for gelation,<sup>15</sup> while polysaccharide chains are also known to aggregate in DMSO.<sup>16</sup> In DMSO at room temperature at 1 wt %, both 16GP-G2 and 28GP-G2 formed organogels that do not flow (Figure 3). Both

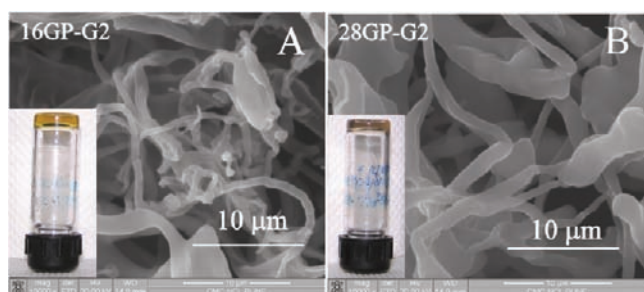


**Figure 3.** SEM images of (A) 16GP-G2 and (B) 28GP-G2 at 1 wt % in DMSO. Insets: corresponding pictures of the gel.

the gels were also analyzed by SEM using freeze-dried assemblies that showed a network of fiber-like structures (Figure 3).

Clear solutions in water, a selective solvent for the GP block, could be prepared by dialysis of 0.1 wt % solutions of the polymer in DMSO:H<sub>2</sub>O (1:1) against deionized water. Initially, water was added dropwise to the solution of polymer in DMSO to induce aggregation of hydrophobic dendron block and formation of the morphology. This was followed by extensive dialysis for complete removal of organic solvent. To visualize the aggregates formed, a drop of the solution was deposited on a carbon-coated grid and analyzed by TEM using uranyl acetate as negative staining agent. 16GP-G1 and 28GP-G2 exhibited

aggregated micellar structures (Figure 4A,C), while 28GP-G1 understandably did not show a well-defined morphology due to

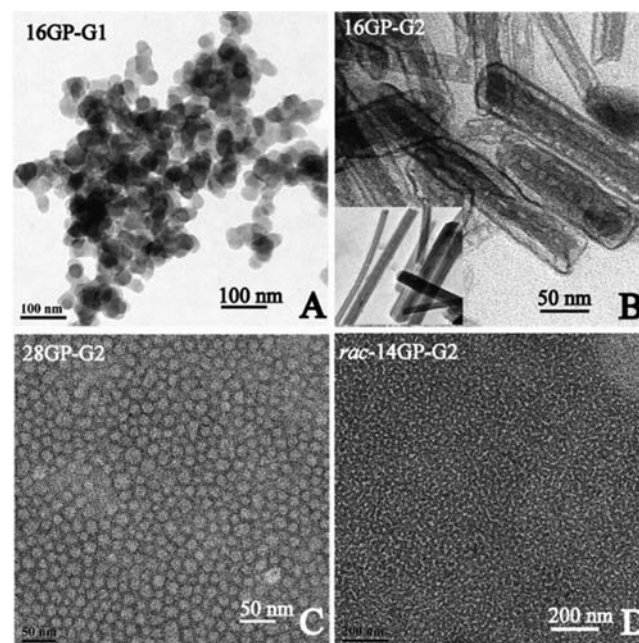


**Figure 4.** TEM images of (A) 16GP-G1, (B) 16GP-G2, (C) 28GP-G2, and (D) *rac*-14GP-G2 in water (0.1 wt %) with uranyl acetate as negative stain.

a higher weight fraction of hydrophilic part (93.7%) (Figure S6A).

The most interesting structures, however, were exhibited by 16GP-G2, which forms rod-like assemblies that are hundreds of nanometers in length, with a uniform width of about 50 nm. For molecules with anisotropic shapes, including dendron–rod–coil and dendron–coil type molecules,<sup>17</sup> formation of nanostructures with high aspect ratio is known; however, our assemblies were found to contain a compartmentalized interior as well when observed under high magnification (Figure 4B). These assemblies are stable in solution, at least up to several weeks. We propose that each self-assembly is primarily directed by relative hydrophobic content, with the GP block forming the hydrophilic exterior and dendrons forming the hydrophobic interior. We estimate that the volume ratio of the hydrophilic rod–coil to the hydrophobic dendron is in accord with the packing parameter arguments for the formation of rod-like structures (Supporting Information, p S24).<sup>18</sup> However, such simple geometric arguments are inadequate to rationalize the formation of compartmentalized structures. The structural rigidity in these systems and the possibility of  $\pi$ – $\pi$  interactions in the wedge segments are likely to contribute to the formation of complex structures such as compartmentalized rods. For 16GP-G2, the weight fraction of dendron is significant (25.7%), whereas for 28GP-G2 it decreases to 17%. Thus, for shorter hydrophilic chains, the molecules are arranged presumably in a curled-up bilayer structure, which may account for the formation of nanorods, whereas for the longer hydrophilic chains, a transition to micelles is favored. To test whether polymers with even shorter hydrophilic chains would form rod-like morphology, a homologue of 16GP-G2 with eight glycopeptide units was synthesized (Figure S6A). It was found to assemble into longer nanofibers, although the polymer

sample itself is polydisperse. Thus, it may be possible to obtain nanorods and nanofibers of predictable dimensions by using dendron-appended monodisperse oligo-glycopeptides of certain chain length. Toward this goal, synthesis of short glycopeptide oligomers with exact numbers of repeat units using solid-phase synthesis is currently being pursued in our laboratory.

It is important to note that the volume fraction of the hydrophilic chains, which influences the self-assembly of these polymers, is in turn influenced by the secondary structure. Helicity in the polypeptide segments will result in a more compact conformation relative to a random coil chain. Further, interchain interactions are also likely to be affected by the polypeptide chain helicity. Thus, a polymer with no secondary structure should exhibit a morphology that is different from the one shown by a polymer with considerable helicity.<sup>19</sup> To test this hypothesis in the case of GP–dendron copolymers, we synthesized a GP of 14 repeat units, by using a racemic mixture of monomers. The CD spectrum of this polymer shows a complete absence of helicity (Figure S3B). An aqueous solution of the dendron conjugate from this polymer, *rac*14GP-G2, where the carbohydrate units are in deprotected form, was then analyzed by TEM. Figure 4D shows that it does not form rod-like morphology, suggesting a strong correlation between secondary structure of the polymer and the resultant self-assembly.

The amphiphatic PEG linker between the GP and dendron is made up of 11 repeat units. To investigate whether it plays a part in the self-assembly of these polymers, we prepared two more polymers based on 16GP polypeptide chain and G2 dendron—one with triethylene glycol linker (16GP-TEG-G2) and the other with heptaethylene glycol linker (14GP-HEG-G2). Self-assembly of the two deprotected polymers was studied in aqueous solutions at 0.1 wt %. TEM images (Figure 5) show that both 16GP-TEG-G2 and 14GP-HEG-G2 form

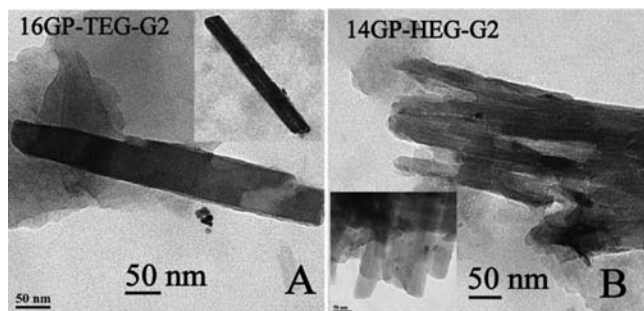


**Figure 5.** TEM images of (A) 16GP-TEG-G2 and (B) 14GP-HEG-G2 in water (0.1 wt %) with uranyl acetate as negative stain.

rod-like morphology. This clearly illustrates that the length of PEG linker does not influence self-assembly of these macromolecules into rod-like structures.

As an additional proof of the presence of micellar assemblies, we carried out dye encapsulation experiments. Nile Red, a hydrophobic dye, was sequestered in the interior of micellar assemblies from 28GP-G2 and the rod-like assemblies from 16GP-G2 in aqueous solutions, as evidenced by a visible change in the color of the solution and also by the fluorescence emission spectrum, which shows a broad peak with  $\lambda_{\text{max}} = 630$  nm when excited at 530 nm (Figures 6 and S8B). This suggests that hydrophobic guest molecules can be loaded into these bioactive micellar assemblies. Similarly, dye encapsulation was also observed with 16GP-G1 (Figure S8C). To determine

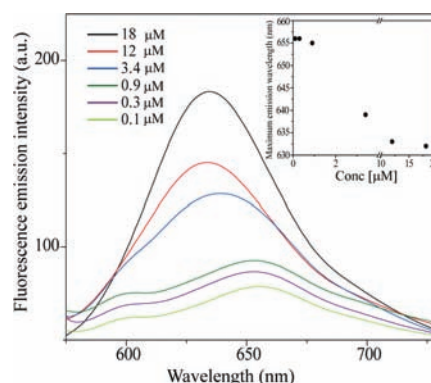


**Figure 6.** Fluorescence emission spectra of Nile Red in aqueous solution of 28GP-G2 at different concentrations of polymer. Inset: plot of  $\lambda_{\text{em}}$  of Nile Red vs concentration of 28GP-G2.

critical micelle concentration (cmc) value for assemblies from 28GP-G2, fluorescence emission spectra of the encapsulated dye at different concentrations of the polymer were recorded by exciting at 530 nm. Around 1  $\mu\text{M}$  concentration, a red shift in the  $\lambda_{\text{max}}$  typical for the emission spectrum of Nile Red in aqueous environment, was observed (Figure 6), and the plot of  $\lambda_{\text{em}}$  of Nile Red vs concentration of polymer has the shape typical for a cmc curve.

**Interaction with Lectins.** Multivalent interactions such as protein–carbohydrate interactions are involved in many biological processes and are known to depend on ligand density and stoichiometry among other factors.<sup>20</sup> Lectins are oligomeric proteins that are involved in cellular signaling via such interactions.<sup>1c,20</sup> Artificial glycoconjugate assemblies that present sugar moieties on the surface in an organized fashion could be used to interrupt undesired protein–carbohydrate interactions. To demonstrate the functional nature of our nanostructures toward this goal, we synthesized D-mannose-containing GP and clicked it to the G2 dendron. This polymer, *manno*14GP-G2, was also found to assemble into rod-like structures in water, as can be seen in TEM micrographs (Figure S6B). To test the possibility that the rod-like morphology does not necessarily depend on isomerism in the sugar residue, we prepared a random copolymer of D-glucose and D-mannose with a 3:1 ratio of glucose and mannose, containing PEG(11)-azide at one end and clicked with G2 dendron alkyne to afford *gluco-manno*(3:1)-14GP-G2. This polymer was found to assemble into nanorods, as observed by TEM analysis (Figure S7A).

To study the response of these mannose-containing nanorods to lectins, we used ConA as a model lectin. The recognition and binding abilities of the mannose-containing nanorods with ConA were estimated by turbidimetric assay, where an increase in turbidity upon addition of nanorods to ConA was observed, indicative of formation of large aggregates (Figure S9). Further, a precipitation assay was performed using a series of dilutions of *manno*14GP-G2 solution at neutral pH. As the concentration of polymer increased, the amount of ConA that precipitated also increased, as evidenced by absorbance at 280 nm characteristic of ConA (Figure 7, plot A). This strongly suggests that carbohydrates on the surface of nanorods are available for interaction with lectins and that these self-assembled structures are functional.

Binding of ConA to glycopolymers with varying numbers of mannose residues has been used to study the effect of epitope



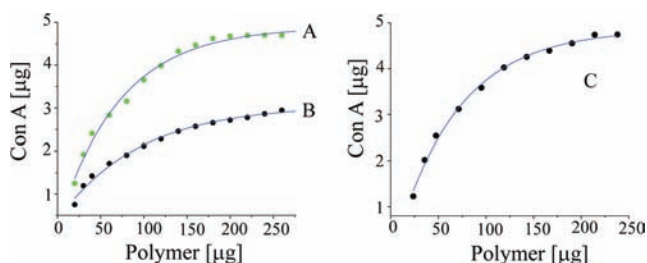


**Figure 7.** Amount of ConA precipitated using various concentrations of (A) *manno*-14GP-G2, (B) *gluco-manno*(3:1)-14GP-G2 rod-like assemblies, and (C) *manno*-28GP-G2 spherical assemblies, as determined by precipitation assay.

density in a multivalent ligand on receptor clustering.<sup>21</sup> The random copolymer of glucose- and mannose-containing repeat units [*gluco-manno*(3:1)-14GP-G2] provides an opportunity to vary the density of functionalities on a self-assembled nanostructure. To study the effect of mannose content on ConA binding, precipitation assays were performed with the nanorods assembled from this polymer (Figure 7, plot B). Plots A and B in Figure 7 show that the amount of precipitated ConA increases with the mannose content in the copolymer, with the amount of precipitated ConA being higher for nanorods displaying only mannose. Thus, lectin binding can be controlled by using the amount of receptor sugar residue on the surface of the assembly. Micellar assemblies from *manno*-28GP-G2 (Figure S7B) were also found to bind to Con A, showing that these micellar assemblies are also functional (Figure 7, plot C).

## CONCLUSION

In summary, we have shown that self-assembled supramolecular structures with a range of one-dimensional to three-dimensional topologies are afforded by amphiphilic glycopolymer-peptide-dendron conjugates based on a single structural motif: a wedge-like dendron attached to stiff GP chains by a coil-like oligo(ethylene glycol). The self-assembly was found to depend upon generation of the dendron, the length of the GP segment, the protected or unprotected form of sugar residue, and the extent of helicity of the polypeptide backbone but was not affected by the length of the PEG linker. The availability of carbohydrate groups on these nanostructures was also demonstrated by lectin binding interaction with ConA. The amount of ConA binding could be varied with mannose content in the self-assembly. Thus, we have clearly illustrated that, in principle, it is possible to design glycoconjugate nanostructures of different shapes for specific interaction with lectins. Further investigations on the underlying mechanism of self-assembly of these polymers and incorporation of biocompatible dendrons are the focus of our future work in this direction.

## ASSOCIATED CONTENT

### Supporting Information

Synthetic procedures for all monomers and polymers with characterization by <sup>1</sup>H and <sup>13</sup>C NMR, FT-IR, and MS; NMR spectra, fluorescence spectra, CD spectra, and SEM and TEM images. This material is available free of charge via the Internet at <http://pubs.acs.org>.

## AUTHOR INFORMATION

### Corresponding Author

av.ambade@ncl.res.in; ss.sengupta@ncl.res.in

### Notes

The authors declare no competing financial interest.

## ACKNOWLEDGMENTS

D.P. and S.D. acknowledge research fellowships from CSIR. N.K. thanks UGC for a fellowship. S.S.G. acknowledges funding from CSIR Network project NWP0051-C. A.V.A. acknowledges financial support from DST, New Delhi, under Fast Track Scheme for Young Scientists via grant number SR/S1/CS-160/2010. We thank Anuya Nisal for help with rheology measurement and Sushma Kumari Singh for SAXS measurements.

## REFERENCES

- (1) (a) Spain, S. G.; Gibson, M. I.; Cameron, N. R. *J. Polym. Sci., Part A: Polym. Chem.* **2007**, *45*, 2059–2072. (b) Schatz, C.; Lecommandoux, S. *Macromol. Rapid Commun.* **2010**, *31*, 1664–1684. (c) Ting, S. R. S.; Chen, G.; Stenzel, M. H. *Polym. Chem.* **2010**, *1*, 1392–1412.
- (2) Boltje, T. J.; Buskas, T.; Boons, G.-J. *Nature Chem.* **2009**, *1*, 611–622.
- (3) (a) You, L.; Schlaad, H. *J. Am. Chem. Soc.* **2006**, *128*, 13336–13337. (b) Schatz, C.; Louguet, S.; Le Meins, J.-F.; Lecommandoux, S. *Angew. Chem., Int. Ed.* **2009**, *48*, 2572–2575. (c) Schlaad, H.; You, L.; Sigel, R.; Smarsly, B.; Heydenreich, M.; Manton, A.; Mašić, A. *Chem. Commun.* **2009**, 1478–1480. (d) Li, Z.-C.; Liang, Y.-Z.; Li, F.-M. *Chem. Commun.* **1999**, 1557–1558. (e) Gress, A.; Smarsly, B.; Schlaad, H. *Macromol. Rapid Commun.* **2008**, *29*, 304–308. (f) Chen, G.; Amajjahe, S.; Stenzel, M. H. *Chem. Commun.* **2009**, 1198–1200.
- (4) (a) Miura, Y. *J. Polym. Sci., Part A: Polym. Chem.* **2007**, *45*, 5031–5036. (b) Dong, C. M.; Sun, X. L.; Faucher, K. M.; Apkarian, R. P.; Chaikof, E. L. *Biomacromolecules* **2004**, *5*, 224–231. (c) Rabuka, D.; Forstner, M. B.; Groves, J. T.; Bertozzi, C. R. *J. Am. Chem. Soc.* **2008**, *130*, 5947–5953. (d) Ruff, Y.; Buhler, E.; Candau, S. J.; Kesselman, E.; Talmon, Y.; Lehn, J.-M. *J. Am. Chem. Soc.* **2010**, *132*, 2573–2584. (e) Suriano, F.; Pratt, R.; Tan, J. P. K.; Wiradharna, N.; Nelson, A.; Yang, Y.-Y.; Dubois, P.; Hedrick, J. L. *Biomaterials* **2010**, *31*, 2637–2645. (f) Vazquez-Dorbatt, V.; Maynard, H. D. *Biomacromolecules* **2006**, *7*, 2297–2302. (g) Spain, S. G.; Albertin, L.; Cameron, N. R. *Chem. Commun.* **2006**, 4198–4200. (h) Kumar, J.; McDowall, L.; Chen, G.; Stenzel, M. H. *Polym. Chem.* **2011**, *2*, 1879–1886.
- (5) Polizzotti, B. D.; Küick, K. L. *Biomacromolecules* **2006**, *7*, 483–490.
- (6) (a) Kramer, J. R.; Deming, T. J. *J. Am. Chem. Soc.* **2012**, *134*, 4112–4115. (b) Lu, H.; Wang, J.; Bai, Y.; Lang, J. W.; Liu, S.; Lin, Y.; Cheng, J. *Nature Commun.* **2011**, *2*, 206–214.
- (7) (a) Aoi, K.; Tsutsumiuchi, K.; Aoki, E.; Okada, M. *Macromolecules* **1996**, *29*, 4456–4458. (b) Shuang, L.; Küick, K. L. *Polym. Chem.* **2011**, *2*, 1513–1522. (c) Kramer, J. R.; Deming, T. J. *J. Am. Chem. Soc.* **2010**, *132*, 15068–15071. (d) Xiao, C.; Zhao, C.; He, P.; Tang, Z.; Chen, X.; Jing, X. *Macromol. Rapid Commun.* **2010**, *31*, 991–997. (e) Tang, H.; Zhang, D. *Polym. Chem.* **2011**, *2*, 1542–1551. (f) Huang, Y.; Zeng, Y.; Yang, J.; Zeng, Z.; Zhu, F.; Chen, X. *Chem. Commun.* **2011**, *47*, 7509–7511. (g) Huang, J.; Habraken, G.; Audouin, F.; Heise, A. *Macromolecules* **2010**, *43*, 6050–6057. (h) Sun, J.; Schlaad, H. *Macromolecules* **2010**, *43*, 4445–4448. (i) Kempe, K.; Neuwirth, T.; Czaplowska, J.; Gottschaldt, M.; Hoogenboom, R.; Schubert, U. S. *Polym. Chem.* **2011**, *2*, 1737–1743.
- (8) The following paper was published during preparation of this manuscript: Huang, J.; Bonduelle, C.; Thévenot, J.; Lecommandoux, S.; Heise, A. *J. Am. Chem. Soc.* **2012**, *134*, 119–122.
- (9) (a) Wurm, F.; Frey, H. *Prog. Polym. Sci.* **2011**, *36*, 1–52. (b) Rosen, B. M.; Wilson, C. J.; Wilson, D. A.; Peterca, M.; Imam, M. R.; Percec, V. *Chem. Rev.* **2009**, *109*, 6275–6540. (c) Palmer, L. C.;

- Stupp, S. I. *Acc. Chem. Res.* **2008**, *41*, 1674–1684. (d) Lim, Y.; Lee, E.; Lee, M. *Angew. Chem., Int. Ed.* **2007**, *46*, 9011–9014. (e) Shao, H.; Parquette, J. R. *Angew. Chem., Int. Ed.* **2009**, *48*, 2525–2528. (f) Kim, K. T.; Winnik, M. A.; Manners, I. *Soft Matter* **2006**, *2*, 957–965. (g) Spaenig, F.; Ruppert, M.; Dannhaeuser, J.; Hirsch, A.; Guldi, D. M. *J. Am. Chem. Soc.* **2009**, *131*, 9378–9388. (h) Peterca, M.; Percec, V.; Dulcey, A. E.; Nummelin, S.; Korey, S.; Ilies, M.; Heiney, P. A. *J. Am. Chem. Soc.* **2006**, *128*, 6713–6720. (i) Lee, H. I.; Lee, J. A.; Poon, Z. Y.; Hammond, P. T. *Chem. Commun.* **2008**, 3726–3728. (j) Tian, L.; Nguyen, P.; Hammond, P. T. *Chem. Commun.* **2006**, 3489–3491. (k) Lim, Y.; Moon, K.-S.; Lee, M. *J. Mater. Chem.* **2008**, *18*, 2909–2918. (l) Yan, J.-J.; Tang, R.-P.; Zhang, B.; Zhu, X.-Q.; Xi, F.; Li, Z.-C.; Chen, E.-Q. *Macromolecules* **2009**, *42*, 8451–8459. (m) Mackay, M. E.; Hong, Y.; Jeong, M.; Tande, B. M.; Wagner, N. J.; Hong, S.; Gido, S. P.; Vestberg, R.; Hawker, C. J. *Macromolecules* **2002**, *35*, 8391–8399. (n) Gitsov, I. *J. Polym. Sci., Part A: Polym. Chem.* **2008**, *46*, 5295–5314.
- (10) (a) Pati, D.; Shaikh, A. Y.; Hotha, S.; Sen Gupta, S. *Polym. Chem.* **2011**, *2*, 805–811. (b) Pati, D.; Shaikh, A.; Das, S.; Nareddy, P. K.; Swamy, M. J.; Hotha, S.; Sen Gupta, S. *Biomacromolecules* **2012**, DOI: 10.1021/bm201813s.
- (11) (a) Zhang, L.; Eisenberg, A. *Science* **1995**, *268*, 1728–1731. (b) Holder, S. J.; Sommerdijk, N. A. J. M. *Polym. Chem.* **2011**, *2*, 1018–1028. (c) Discher, D. E.; Eisenberg, A. *Science* **2002**, *297*, 967–973. (d) Blanz, A.; Armes, S. P.; Ryan, A. J. *Macromol. Rapid Commun.* **2009**, *30*, 267–277.
- (12) (a) Tornøe, C. W.; Christensen, C.; Meldal, M. *J. Org. Chem.* **2002**, *67*, 3057–3064. (b) Meldal, M.; Wenzel, C.; Tornøe, C. W. *Chem. Rev.* **2008**, *108*, 2952–3015. (c) Kolb, H. C.; Finn, M. G.; Sharpless, K. B. *Angew. Chem., Int. Ed.* **2001**, *40*, 2004–2021. (d) Iha, R. K.; Wooley, K. L.; Nystrom, A. M.; Burke, D. J.; Kade, M. J.; Hawker, C. J. *Chem. Rev.* **2009**, *109*, 5620–5686. (e) Binder, W. H.; Sachsenhofer, R. *Macromol. Rapid Commun.* **2007**, *28*, 15–54. (f) Kempe, K.; Krieg, A.; Becer, C. R.; Schubert, U. S. *Chem. Soc. Rev.* **2012**, *41*, 176–191. (g) Hua, C.; Peng, S.-M.; Dong, C.-M. *Macromolecules* **2008**, *41*, 6686–6695. (h) Laurent, B. A.; Grayson, S. M. *J. Am. Chem. Soc.* **2006**, *128*, 4238–4239.
- (13) (a) Hanson, J. A.; Li, Z.; Deming, T. J. *Macromolecules* **2010**, *43*, 6268–6269. (b) Bellomo, E. G.; Wyrsta, M. D.; Pakstis, L.; Pochan, D. J.; Deming, T. J. *Nat. Mater.* **2004**, *3*, 244–248.
- (14) Foster, T.; Safran, S. A.; T. Sottmann, T.; Strey, R. *J. Chem. Phys.* **2007**, *127*, 204711/1–204711/16.
- (15) (a) Duan, P.; Zhu, X.; Liu, M. *Chem. Commun.* **2011**, *47*, 5569–5571. (b) Deng, W.; Thompson, D. H. *Soft Matter* **2010**, *6*, 1884–1887. (c) George, M.; Snyder, S. L.; Terech, P.; Glinka, C. J.; Weiss, R. G. *J. Am. Chem. Soc.* **2003**, *125*, 10275–10283. (d) Jung, J. H.; Kobayashi, H.; Masuda, M.; Shimizu, T.; Shinkai, S. *J. Am. Chem. Soc.* **2001**, *123*, 8785–8789. (e) Seo, S.-H.; Park, J.-H.; Chang, J.-Y. *Langmuir* **2009**, *25*, 8439–8441.
- (16) Östlund, A.; Lundberg, D.; Nordstierna, L.; Holmberg, K.; Nydén, M. *Biomacromolecules* **2009**, *10*, 2401–2407.
- (17) (a) Kim, J.-K.; Lee, E.; Lee, M. *Angew. Chem., Int. Ed.* **2006**, *45*, 7195–7198. (b) Zubarev, E. R.; Pralle, M. U.; Sone, E. D.; Stupp, S. I. *J. Am. Chem. Soc.* **2001**, *123*, 4105–4106. (c) Park, C.; Lee, I. H.; Lee, S.; Song, Y.; Rhue, M.; Kim, C. *Proc. Natl. Acad. Sci. U.S.A.* **2006**, *103*, 1199–1203. (d) Cornelissen, J. J. L. M.; van Heerbeek, R.; Kamer, P. C. J.; Reek, J. N. H.; Sommerdijk, N. A. J. M.; Nolte, R. J. M. *Adv. Mater.* **2002**, *14*, 489–492.
- (18) Israelachvili, J. N. *Intermolecular and Surface Forces*, 2nd ed; Academic Press: San Diego, 1991.
- (19) (a) Chécot, F.; Lecommandoux, S.; Gnanou, Y.; Klok, H.-A. *Angew. Chem., Int. Ed.* **2002**, *41*, 1339–1343. (b) Klok, H.-A.; Langenwalter, J. F.; Lecommandoux, S. *Macromolecules* **2000**, *33*, 7819–7826. (c) Schneider, J. P.; Pochan, D. J.; Bulent, O.; Karthikan, R.; Pakstis, L.; Kretsinger, J. *J. Am. Chem. Soc.* **2002**, *124*, 15030–15037. (d) Ghosh, A.; Haverick, M.; Stump, K.; Yang, X.; Tweedle, M. F.; Goldberger, J. E. *J. Am. Chem. Soc.* **2012**, *134*, 3647–3650.
- (20) Liu, S.; Kiick, K. *Macromolecules* **2008**, *41*, 764–772.
- (21) (a) Admiral, V.; Mantovani, G.; Clarkson, G. J.; Cauet, S.; Irwin, J. L.; Haddleton, D. M. *J. Am. Chem. Soc.* **2006**, *128*, 4823–